

# Accurate Determination of Modes in Dielectric-Loaded Cylindrical Cavities Using a One-Dimensional Finite Element Method

M. MOHAMMAD TAHERI AND D. MIRSHEKAR-SYAHKAL

**Abstract**—A unified approach is presented here to calculate the resonant frequencies of all the modes in cylindrical cavities axisymmetrically loaded with dielectrics. In this method, the radial variations of the field components in the resonator are expressed in terms of first-degree finite element polynomials while the axial variations of the field components are approximated by trigonometric functions. To calculate the resonant frequencies, an  $H$ -vector variational formulation is employed and minimized with respect to the coefficients of the expanded field components. Spurious solutions which are inherent in the finite element technique are effectively eliminated by means of a penalty term included in the variational expression, imposing a divergence-free magnetic field constraint. To show the capability of the method, resonant frequencies of several cylindrical cavities including those loaded with dielectric rods and dielectric rings were calculated. A mode chart is also presented which can be used for designing certain multimode dielectric-loaded cavity filters. In contrast to other rigorous techniques reported in the literature, the present method is highly efficient when dielectrics are fully extended along the cavity length.

## I. INTRODUCTION

IT IS WELL established that the design of multimode dielectric-loaded cavity filters [1], [2] requires an accurate specification of the degenerate modes of dielectric-loaded cavity resonators. The work described in this paper has originated from a need for a flexible but powerful method of determining all modes in cylindrical cavities loaded axisymmetrically with several dielectrics (Fig. 1). A study revealed that the existing methods of analysis of dielectric-loaded cylindrical cavities suffer from various shortcomings. These methods either become mathematically complex when several dielectrics are involved in the structure of the resonator [3]–[6] or they are not applicable to the determination of all the categories of modes (TE, TM, and hybrids) [7], [8]. One method, reported in [9], which can conveniently deal with all the modes is, however, found not to satisfy our requirements on the grounds that it uses a two-dimensional finite element method; hence it cannot be economical when dealing with dielectrics fully extended along the cavity.

For calculating the resonant frequencies of dielectric-loaded cavity resonators of the general configuration shown

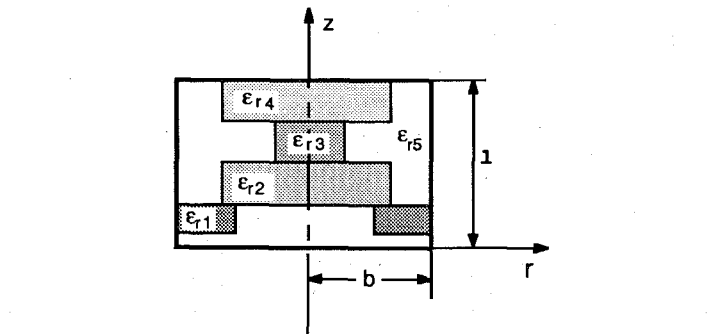


Fig. 1. Cross section of a cylindrical cavity resonator axisymmetrically loaded with dielectrics.

in Fig. 1, as in [9], we started with the well-known  $H$ -vector variational expression [10]:

$$\omega^2 = \frac{\iiint (\nabla \times \mathbf{H}) \epsilon^{-1} (\nabla \times \mathbf{H})^* dv}{\iiint \mathbf{H} \mu \mathbf{H}^* dv} \quad (1)$$

where the asterisk denotes the complex conjugate,  $\omega$  is the angular resonant frequency,  $\mathbf{H}$  is the magnetic field inside the cavity, and the integrals are performed over the volume of the cavity. For the problems of concern, the  $H$  formulation (1) is advantageous over other variational expressions for two main reasons. First, for an arbitrary metallic resonator the requirement of the tangential electric field is automatically satisfied [10]. Second, since the magnetic field is continuous at the interface of two dielectrics, no special treatment of dielectric boundaries is necessary for any number of dielectrics involved in the cavity.

In this paper, initially an efficient method for determining  $\omega$  from (1) is described. The method is then tested by computing the resonant frequencies of several dielectric-loaded cavities for which solutions are available by other techniques.

## II. METHOD OF SOLUTION

Application of (1) requires that the magnetic field  $\mathbf{H}$  be expressed in terms of a set of basis functions. Since the resonator of Fig. 1 is axisymmetrical, the variation of the

Manuscript received November 3, 1988; revised April 11, 1989.

The authors are with the Department of Electronic Systems Engineering, University of Essex, Wivenhoe Park, Colchester, CO4 3SQ, U.K.  
IEEE Log Number 8929886.

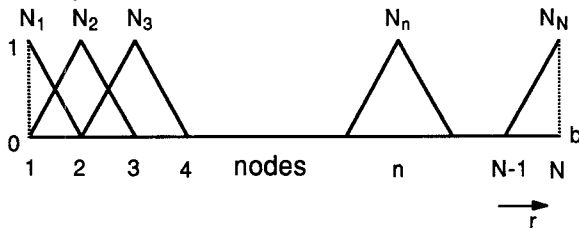


Fig. 2. First-order finite element basis functions.

magnetic field along the  $\theta$  direction is sinusoidal [11]. Thus, components of  $\mathbf{H}$  can be expressed as

$$H_z = \begin{cases} \cos(m\theta) \\ \sin(m\theta) \end{cases} f(r, z) \quad (2a)$$

$$H_r = \begin{cases} \cos(m\theta) \\ \sin(m\theta) \end{cases} g(r, z) \quad (2b)$$

$$H_\theta = \begin{cases} \sin(m\theta) \\ \cos(m\theta) \end{cases} h(r, z) \quad (2c)$$

where, depending on the mode,  $m$  is  $0, 1, 2, \dots$ . The functions  $f(r, z)$ ,  $g(r, z)$ , and  $h(r, z)$  can be defined generally by many complete sets of basis functions. Since the outer boundary is always cylindrical, an efficient representation of the magnetic field is

$$H_z = \begin{cases} \cos(m\theta) \\ \sin(m\theta) \end{cases} \sum_{p=1}^{P+1} \sum_{n=1}^N A_{np} N_n(r) \sin\left(\frac{p\pi}{l} z\right) \quad (3a)$$

$$H_r = \begin{cases} \cos(m\theta) \\ \sin(m\theta) \end{cases} \sum_{p=0}^P \sum_{n=1}^N B_{np} N_n(r) \cos\left(\frac{p\pi}{l} z\right) \quad (3b)$$

$$H_\theta = \begin{cases} \sin(m\theta) \\ \cos(m\theta) \end{cases} \sum_{p=0}^P \sum_{n=1}^N C_{np} N_n(r) \cos\left(\frac{p\pi}{l} z\right) \quad (3c)$$

where  $l$  is the cavity length. The advantage of the above expansions becomes conspicuous in computations where all the dielectrics fully occupy the cavity length, in which case they reduce to one-dimensional expansions in terms of  $N_n(r)$ .

The resonant frequencies and expansion coefficients  $(A_{np}, B_{np}, C_{np})$  can be obtained from a matrix equation resulting from the application of the Rayleigh-Ritz procedure to the functional defined for the problem [11]. From the computing point of view, it is advantageous to have sparse matrices involved in this equation. One way of achieving this is to use a one-dimensional finite element technique for approximating the radial behavior of the field. The structure in the radial direction is discretized into elements consisting of two nodes. A first-degree polynomial in  $r$  with a value of 1 at the  $n$ th node and zero at others (Fig. 2) is then associated with  $N_n(r)$ . This arrangement not only produces sparsity in the final matrices; it also greatly facilitates the integration task involved in (1) when several dielectrics are contained in the resonator.

In the present variational formulation, (1), solutions satisfy boundary conditions automatically (see Section I) whereas they do not meet the condition  $\nabla \cdot \mathbf{H} = 0$ , resulting

in the generation of spurious modes [9], [12], [13]. By adding a penalty term [14] to (1), however, one can enforce the divergence-free constraint on  $\mathbf{H}$ . The variational expression including the penalty term is

$$\omega^2 = \frac{\iiint (\nabla \times \mathbf{H}) \epsilon^{-1} (\nabla \times \mathbf{H})^* dv + S \iiint |\nabla \cdot \mathbf{H}|^2 dv}{\iiint \mathbf{H} \mu \mathbf{H}^* dv} \quad (4)$$

where  $S$  is the penalty parameter. By assuming  $S = 0$ , (4) reduces to (1). For physical modes,  $\nabla \cdot \mathbf{H} = 0$  and hence these solutions should be independent of the values of  $S$ . When the expanded forms, (3), of the magnetic field components are substituted into (4), the result can be stated as

$$\omega^2 = \frac{\mathbf{N}(A_{np}, B_{np}, C_{np}, S)}{\mathbf{D}(A_{np}, B_{np}, C_{np})}. \quad (5)$$

The Rayleigh-Ritz method [11], [14] can now be applied to (5) to compute  $A_{np}$ ,  $B_{np}$ ,  $C_{np}$ , and  $\omega$ . This method generates a set of linear algebraic eigenvalue equations

$$[Q][x] = k^2 [R][x] \quad (6)$$

where  $k^2 = \omega^2 \mu_0 \epsilon_0$  and  $[x]$  is a column matrix consisting of  $A_{np}$ ,  $B_{np}$ , and  $C_{np}$ . The matrices  $[Q]$  and  $[R]$  are very sparse and their densities can be proved to be

$$S_Q = 3S_R = \frac{(3N-2)}{N^2} \quad (7)$$

where  $N$  is the number of nodes and  $S_Q$  and  $S_R$  are the ratios of the number of nonzero elements to the total number of elements in the matrices  $[Q]$  and  $[R]$  respectively.

### III. NUMERICAL RESULTS

The eigenvalue equation (6) has been solved by a standard subroutine [15] to obtain the eigenvalues (resonant frequencies) and eigenvectors (field coefficients).

To check the capability of the penalty term in removing spurious modes, we have initially computed resonant frequencies of angular dependent modes ( $TE_{mnp}$  and  $TM_{mnp}$ ) of an empty cylindrical cavity for which analytical expressions are available. For the  $TE$  modes, all three components of the magnetic field are nonzero and hence the maximum number of components is involved in computations. The results of the test are presented in Table I. From this table, it is seen that as the penalty parameter  $S$  increases, the number of spurious modes eliminated rises. In fact, by increasing  $S$ , the spurious solutions move down in the spectrum of the eigenvalues. Introducing the penalty term does, however, change the resonant frequency of physical modes slightly [13]. Fig. 3 shows this fact for the  $TE_{111}$  and  $TM_{111}$  modes as  $S$  increases. Further numerical checks were also performed in order to establish confidence in the accuracy of the present technique [16].

TABLE I  
THE VARIATION OF THE SPECTRUM OF MODES AS THE PENALTY  
PARAMETER  $S$  INCREASES: SP INDICATES A SPURIOUS MODE

Eigenvalue No.	$10^{-10}S$								
	0	3.96	6.22	14.1	28.2	50.9	67.8	113	339
1	SP	SP	SP	$TE_{111}$	$TE_{111}$	$TE_{111}$	$TE_{111}$	$TE_{111}$	$TE_{111}$
2	SP	$TE_{111}$	$TE_{111}$	SP	SP	$TM_{111}$	$TM_{111}$	$TM_{111}$	$TM_{111}$
3	SP	SP	SP	$TM_{111}$	$TM_{111}$	$TE_{121}$	$TE_{121}$	$TE_{121}$	$TE_{121}$
4	SP	$TM_{111}$	$TM_{111}$	$TE_{121}$	SP	SP	$TM_{121}$	$TM_{121}$	$TM_{121}$
5	SP	SP	$TE_{121}$	SP	$TE_{121}$	$TM_{121}$	$TM_{121}$	SP	$TE_{131}$
6	SP	$TE_{121}$	SP	$TM_{121}$	$TM_{121}$	$TE_{131}$	$TE_{131}$	$TE_{131}$	$TM_{131}$
7	SP	SP	$TM_{121}$	$TE_{131}$	$TE_{131}$	$TM_{131}$	$TM_{131}$	$TM_{131}$	$TE_{131}$
8	SP	$TM_{121}$	$TE_{131}$	SP	SP	$TE_{141}$	$TE_{141}$	$TE_{141}$	$TM_{141}$
9	SP	SP	$TM_{131}$	$TM_{131}$	$TM_{131}$	SP	$TM_{141}$	$TM_{141}$	
10	SP	$TE_{131}$	$TM_{131}$	$TE_{141}$	$TE_{141}$	$TM_{141}$			
11	SP	SP	SP	$TM_{141}$					
12	SP	$TM_{131}$	$TE_{141}$	$TM_{141}$					
13	SP	$TE_{141}$	$TM_{141}$						
14	SP	SP							
15	SP	$TM_{141}$							

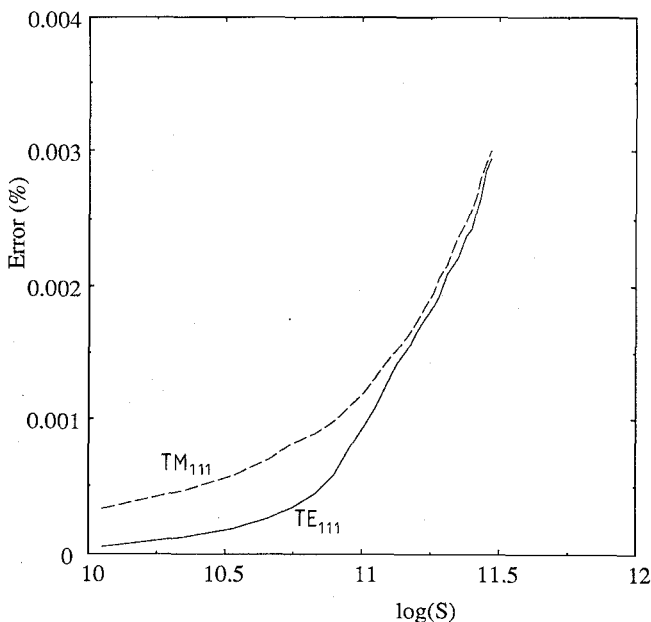


Fig. 3. Typical error in the computation of the resonant frequencies of  $TE_{111}$  and  $TM_{111}$  modes of an empty cylindrical cavity against the value of the penalty parameter  $S$ .

The resonator in Fig. 4(a) has wide applications in the design of multimode filters [1], [17]. In its simplest form, the dielectric in the resonator extends fully along the cavity length (Fig. 4(b)). In this case, the axial function of the field can be expressed by only one sinusoidal term in (3). Table II compares the computed resonant frequencies for the first four modes against the results of mode matching [18] for a cylindrical cavity resonator loaded with a dielectric rod ( $\epsilon_r = 37.6$ ,  $a = 0.394$  in,  $b = 0.5$  in). An excellent agreement between the two techniques is evident.

For the resonator shown in Fig. 4(a) when the dielectric is symmetrically located in the cavity (i.e.,  $l_1 = l_2$ ), the axial function of the field is not sinusoidal. Hence, the number of axial terms  $P \geq 1$ . For a specific resonator ( $\epsilon_r = 37.6$ ,  $b/a = 1.25$ ,  $a = 4$  mm,  $l/h = 3$ ) curves representing the convergence of the resonant frequencies of the first three modes are computed and depicted in Fig. 5. It is

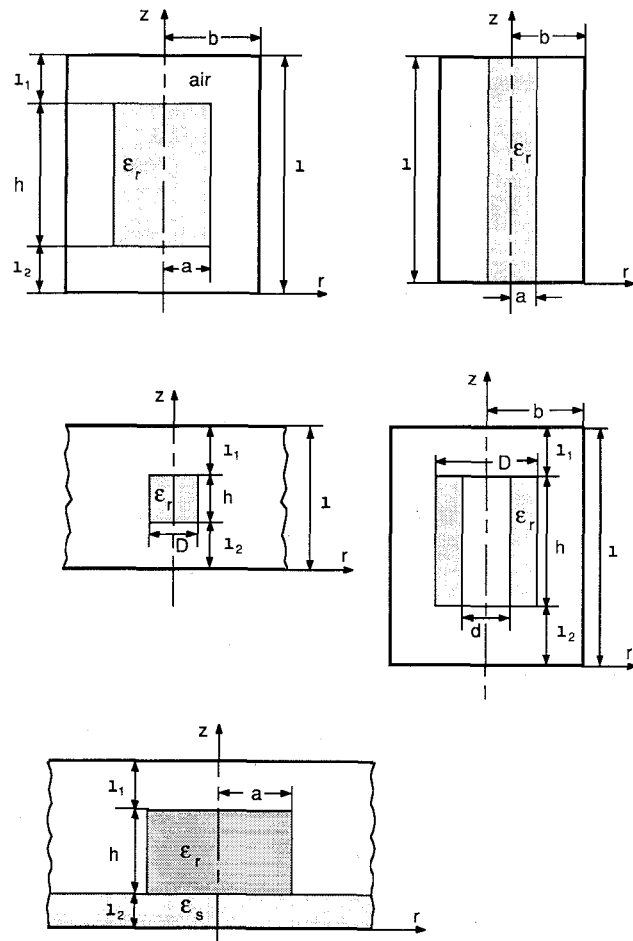


Fig. 4. Cross sections of resonators analyzed in this paper.

TABLE II  
COMPARISON OF RESONANT FREQUENCIES (GHz) COMPUTED  
BY THE PRESENT TECHNIQUE AND THOSE GIVEN IN [18]  
FOR A CYLINDRICAL CAVITY LOADED WITH  
A DIELECTRIC ROD

$(D/l)^2$	$HE_{111}$		$HE_{121}$		$TM_{011}$		$HE_{211}$	
	Ref[18]	Present Tech.						
2	2.494	2.489	3.820	3.813	3.363	3.380	3.391	3.402
3	2.750	2.758	4.078	4.040	3.582	3.613	3.534	3.541
4	3.006	3.015	4.246	4.237	3.802	3.824	3.715	3.742
5	3.253	3.250	4.395	4.389	4.013	4.020	3.930	3.961
6	3.458	3.467	4.600	4.607	4.189	4.205	4.118	4.135
7	3.670	3.682	4.791	4.780	4.403	4.381	4.313	4.330
8	3.888	3.879	4.936	4.951	4.550	4.550	4.463	4.491
9	4.081	4.067	5.098	5.099	4.710	4.713	4.622	4.661

For Fig. 4(b),  $\epsilon_r = 37.6$ ,  $b = 0.5$  in,  $a = 0.394$  in, and  $D = 2a$ . Note that values from [18] are correct to within the readability of the curves.

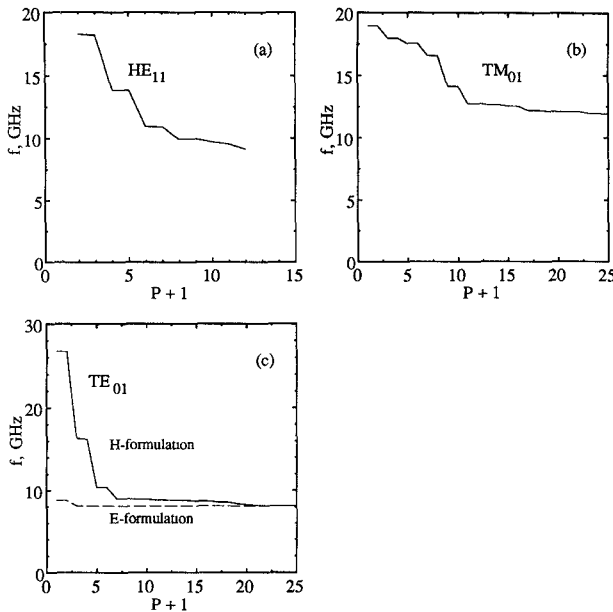


Fig. 5. Convergence of the resonant frequencies of  $HE_{11}$ ,  $TM_{01}$ , and  $TE_{01}$  modes of a cylindrical resonator loaded with a short cylindrical dielectric (Fig. 4(a)):  $\epsilon_r = 37.6$ ,  $l/h = 3$ ,  $a = 4$  mm,  $b/a = 1.25$ , and  $l_1 = l_2$ . In this figure  $P + 1$  shows the number of axial terms in (3) used in the computation.

found that in the special case of  $TE_{0n}$ , a rapid convergence can be obtained if the  $E$ -vector variational expression given in [10] is used (Fig. 5(c)). This effect can be attributed to the fact that the basis functions employed in the solution satisfy more Dirichlet boundary conditions [19] than those utilized in the  $H$ -vector variational expression (4). However, for reasons described before, the  $E$ -vector variational expression is not convenient enough for the purpose of determining the TM and hybrid modes of a dielectric-loaded cavity. It is also found that as the ratio of  $l/h$  increases,  $P$  should be increased in order to maintain the accuracy of the results.

The modes in the dielectric-loaded cavities with symmetrical structures along the  $z$  axis (see the previous example) can be generally grouped into two sets of modes [20]; the modes for which the transverse electric field components are zero at the symmetry plane,  $z = l/2$  (electric wall), and those for which the transverse components of the magnetic field vanish at the same symmetry plane (magnetic wall). In [20], by considering the above symmetry conditions, mathematical formulations are significantly reduced with the consequence of saving a great deal of computer time. In the present technique, however, there is no need to include this symmetry condition in the formulation as the evaluation of the integrals involved in (4) is straightforward. For a cavity resonator loaded with a dielectric disk (Fig. 4(a)) Table III compares resonant frequencies computed by the present technique with those given in [20]. To facilitate the mode designation for cavity resonators with dielectrics not fully occupying the length of the cavity, we followed a mode designation similar to that given by [20]. However, since the even and odd symmetry can be automatically taken care of by the present technique, we have

TABLE III  
COMPARISON OF RESONANT FREQUENCIES (GHZ)  
COMPUTED BY THE PRESENT TECHNIQUE AND  
THOSE GIVEN IN [20] FOR A CYLINDRICAL  
CAVITY LOADED WITH A DIELECTRIC DISK

Mode	Present Tech.	Ref[20]
$TE_{01}$	3.435	3.428 ( $TEH_{01}$ )
$TE_{02}$	5.493	5.462 ( $TEE_{01}$ )
$TM_{01}$	4.601	4.551 ( $TME_{01}$ )
$HE_{11}$	4.271	4.224 ( $HEH_{11}$ )
$HE_{12}$	4.373	4.326 ( $HEE_{11}$ )

For Fig. 4(a),  $\epsilon_r = 35.74$ ,  $h = 0.3$  in,  $l = 0.6$  in,  $a = 0.34$  in,  $b/a = 1.5$ , and  $l_1 = l_2$ . Note that values from [20] are correct to within the readability of the curves.

TABLE IV  
COMPARISON OF RESONANT FREQUENCIES (GHZ) CALCULATED  
BY THE PRESENT TECHNIQUE AND THOSE GIVEN IN [21]–[23]  
FOR  $TE_{01}$  MODE (CONVENTIONALLY KNOWN AS  $TE_{018}$ )  
OF SEVERAL PARALLEL-PLATE RESONATORS LOADED  
WITH SHORT CYLINDRICAL DIELECTRIC

D	h	$l_1/h$	Computed			Measured Ref[21]
			Ref[22]	Ref[23]	Present Tech.	
4.06	5.15	0.568	10.86	10.50	10.53	10.48
6.03	4.16	0.820	8.31	7.94	7.95	7.94
5.98	2.95	1.360	9.16	8.61	8.64	8.64
6.02	2.14	2.070	10.08	9.33	9.36	9.40
7.99	2.14	2.070	8.38	7.76	7.87	7.79

For Fig. 4(c),  $\epsilon_r = 36.2$ ,  $l_1 = l_2$ . All dimensions are in mm.

omitted the even and odd subscripts from the mode designation introduced in [20]. Therefore, the modes are defined as  $TE_{0n}$ ,  $TM_{0n}$ , and  $HE_{mn}$  where the first subscript denotes the angular dependence of the field and the second is the order of the resonant frequency. In the present technique, the even-mode symmetry and the odd-mode symmetry can be easily detected by examining the pattern of the eigenvectors ( $A_{np}$ ,  $B_{np}$ ,  $C_{np}$ ). In Table IV, we have recorded the results of the computation of the resonant frequencies of the  $TE_{01}$  mode (conventionally known as  $TE_{018}$ ) associated with several dielectric resonators of different sizes located symmetrically between two infinite sheets of perfect conductors (Fig. 4(c)). Theoretical and experimental resonant frequencies of these resonators are given in [21]–[23] and are also included in Table IV. The agreement between the resonant frequencies computed by the present technique and those given in [20]–[23] is excellent. In the computation of the resonant frequencies presented in Table IV, we assumed that a cylindrical metallic

TABLE V  
COMPARISON OF RESONANT FREQUENCIES (GHz)  
CALCULATED BY THE PRESENT TECHNIQUE AND  
THOSE GIVEN IN [6] FOR A CYLINDRICAL  
CAVITY LOADED WITH A DIELECTRIC RING

Mode	Present Tech.	Ref[6]
$TE_{01}$	6.64	6.64 ( $TE_{018}$ )
$TE_{02}$	10.49	10.50 ( $TE_{018}$ )
$TM_{01}$	8.42	8.38 ( $TM_{018}$ )
$HE_{11}$	8.86	8.79 ( $HE_{118}$ )
$HE_{12}$	9.84	9.78 ( $HE_{118}$ )

For Fig. 4(d),  $\epsilon_r = 37.5$ ,  $h = 4.124$  mm,  $l = 6.124$  mm,  $d = 3.044$  mm,  $D = 9.051$  mm,  $b = 7.22$  mm, and  $l_1 = l_2$ . Note that values from [6] are correct to within the readability of the curves.

boundary at  $r = 4a$  encloses the structure shown in Fig. 4(c). It is found that when this boundary is at this position or further away, the calculated resonant frequencies are hardly affected. Also note that although results by [22] are acceptable, they are not accurate on the grounds that the associated method of solution is approximate.

To test the generality of the present method, we have also calculated the resonant frequencies of a cylindrical cavity loaded with a dielectric ring (Fig. 4(d)). The resonant frequencies of the first few modes are recorded in Table V together with those reported in [6] for the same structure. Comparing the results, excellent agreement is evident between the two methods.

The general configuration of a dielectric resonator located on a microstrip line substrate is shown in Fig. 4(e). This resonator can be analyzed by the present method if it is assumed that a cylindrical conductor encloses the structure. For a particular resonator ( $\epsilon_r = 38$ ,  $a = h = 4$  mm,  $l_1 = 3$  mm,  $l_2 = 0.79$  mm, and  $\epsilon_s = 2.33$ ), we have computed the resonant frequencies of the first few modes of the structure. In this analysis, we assumed that a cylindrical metallic boundary at  $r = 4a$  encloses the structure. The results of the computation are shown in Table VI together with those given by [4] for comparison.

A mode chart computed by the present technique for a cavity loaded symmetrically with a hollow cylindrical dielectric ( $\epsilon_r = 37$ ,  $b = 18$  mm,  $D = 20$  mm,  $d = 5$  mm) is shown in Fig. 6.

#### IV. CONCLUSION

A unified technique is presented for the computation of the resonant frequencies of all the modes in a cylindrical cavity loaded axisymmetrically with dielectrics. The technique is based on an  $H$ -vector variational expression using first-degree finite element basis functions to represent the radial variation of the field components. It was shown that spurious modes can be effectively removed from the spec-

TABLE VI  
COMPARISON OF RESONANT FREQUENCIES (GHz) COMPUTED  
BY THE PRESENT TECHNIQUE AND THOSE GIVEN IN [4]  
FOR A DIELECTRIC RESONATOR LOCATED ON A  
MICROSTRIP LINE SUBSTRATE

Mode	Present Tech.	Ref[4]
$TE_{01}$	6.82	6.73 ( $TE_{018}$ )
$TE_{02}$	10.79	-
$TE_{03}$	12.09	12.10 ( $TE_{028}$ )
$TM_{01}$	9.51	9.40 ( $TM_{018}$ )
$TM_{02}$	13.10	-
$TM_{03}$	14.72	14.71 ( $TM_{028}$ )

For Fig. 4(e),  $\epsilon_r = 38$ ,  $\epsilon_s = 2.33$ ,  $a = h = 4$  mm,  $l_1 = 3$  mm, and  $l_2 = 0.79$  mm.

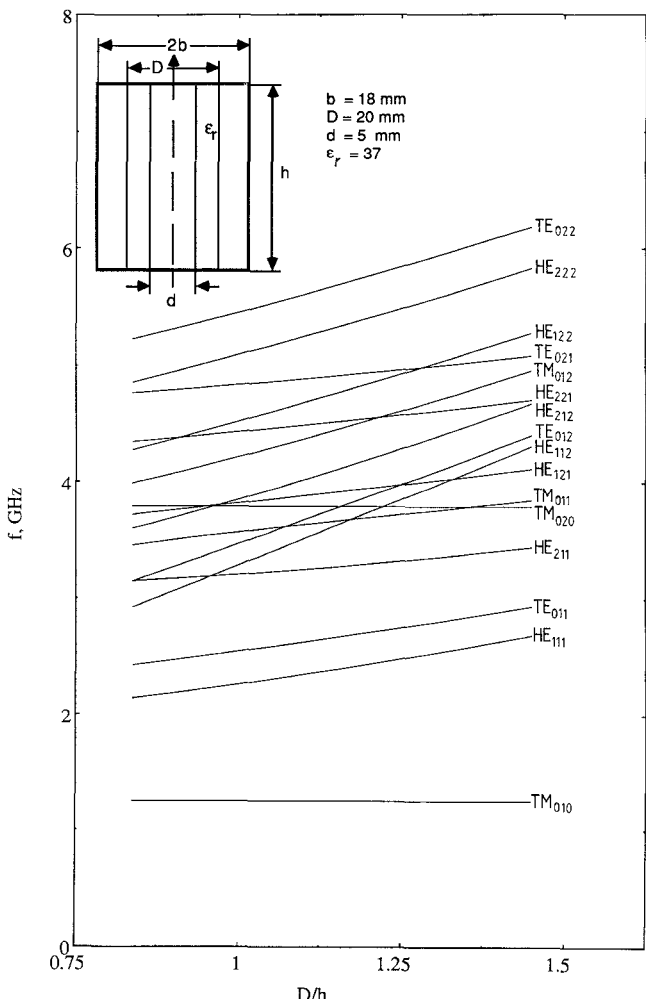


Fig. 6. Mode chart for a cylindrical cavity resonator loaded with a hollow cylindrical dielectric.

trum of physical modes by adding a penalty term to the variational expression. This penalty term imposes the condition of divergence-free magnetic field. The capability of the technique was checked by applying the technique to various dielectric-loaded cavity resonators whose resonant frequencies are already available in the literature. The technique is proved to be very versatile, accurate, and computationally efficient, particularly when dielectrics are the same length as the cavity. Finally, a mode chart computed by the present technique is presented which can be used in the design of certain multimode filters.

## REFERENCES

- [1] S. J. Fiedziuszko, "Dual-mode dielectric resonator loaded cavity filters," *IEEE Trans. Microwave Theory Tech.*, vol. MTT-30, pp. 1311-1316, Sept. 1982.
- [2] D. Siu, "Realization of an exact 5-pole elliptic function filter employing dielectric-loaded triple-dual-mode cavity structure," *IEEE MTT-S Int. Microwave Symp. Dig.*, 1986, pp. 357-359.
- [3] S. Vigneron and P. Guillou, "Mode matching method for determination of the resonant frequency of a dielectric resonator placed in a metallic box," *Proc. Inst. Elec. Eng.*, pt. H, vol. 134, no. 2, pp. 151-155, Apr. 1987.
- [4] L. A. Bermudez and P. Y. Guillon, "Application of variational principle for calculation of resonant frequencies of cylindrical dielectric resonators," *Electron Lett.*, vol. 22, no. 1, pp. 31-33, Jan. 1986.
- [5] K. A. Zaki and A. Atia, "Modes in dielectric-loaded waveguides and resonators," *IEEE Trans. Microwave Theory Tech.*, vol. MTT-31, pp. 1039-1044, Dec. 1983.
- [6] Y. Kobayashi and M. Miura, "Optimum design for shielded dielectric rod and ring resonators for obtaining best mode separation," *IEEE MTT-S Int. Microwave Symp. Dig.*, 1984, pp. 184-186.
- [7] P. S. Kooi, M. S. Leong, and A. L. Satya Parkash, "Finite-element analysis of the shielded cylindrical dielectric resonator," *Proc. Inst. Elec. Eng.*, pt. H, vol. 132, pp. 7-16, Feb. 1985.
- [8] F. H. Gil and J. Perez, "Analysis of dielectric resonators with tuning screw and supporting structure," *IEEE MTT-S Int. Microwave Symp. Dig.*, 1985, pp. 485-488.
- [9] J. B. Davies, F. A. Fernandez, and G. Y. Philippou, "Finite element analysis of all modes in cavities with circular symmetry," *IEEE Trans. Microwave Theory Tech.*, vol. MTT-30, pp. 1975-1980, Nov. 1982.
- [10] A. D. Berk, "Variational principle for electromagnetic resonators and waveguides," *IRE Trans. Antennas Propagat.*, vol. AP-4, pp. 104-111, Apr. 1956.
- [11] R. E. Collin, *Field Theory of Guided Waves*. New York: McGraw Hill, 1960.
- [12] B. M. A. Rahman and J. B. Davies, "Penalty function improvement of waveguide solution by finite element," *IEEE Trans. Microwave Theory Tech.*, vol. MTT-32, pp. 922-928, Aug. 1984.
- [13] J. R. Winkler and J. B. Davies, "Elimination of spurious modes in finite element analysis," *J. Comput. Phys.*, vol. 56, pp. 1-14, Oct. 1984.
- [14] O. C. Zienkiewicz and K. Morgan, *Finite Elements and Approximation*. New York: Wiley, 1983.
- [15] Numerical Algorithms Group (NAG), *Fortran Library Manual*, Mark 11 vol. 4, Oxford, UK, 1984.
- [16] D. Mirshekar-Syahkal and M. Mohammad Taheri, "Unified approach to determination of modes in cylindrical cavity axisymmetrically loaded with dielectrics," *Electron. Lett.*, vol. 23, no. 22, pp. 1177-1178, Oct. 1987.
- [17] W. C. Tang, J. Sferrazza, B. Beggs, and D. Siu, "Dielectric resonator output multiplexer for C-band satellite applications," *IEEE MTT-S Int. Microwave Symp. Dig.*, 1985, pp. 343-345.
- [18] K. A. Zaki and C. Chen, "Loss mechanism in dielectric-loaded resonators," *IEEE Trans. Microwave Theory Tech.*, vol. MTT-33, pp. 1448-1452, Dec. 1985.
- [19] W. J. English and F. J. Young, "An *E*-vector variational formulation of Maxwell equations for cylindrical waveguide problems," *IEEE Trans. Microwave Theory Tech.*, vol. MTT-19, pp. 40-46, Jan. 1971.
- [20] K. A. Zaki and C. Chen, "New results in dielectric-loaded resonators," *IEEE Trans. Microwave Theory Tech.*, vol. MTT-34, pp. 815-824, July 1986.
- [21] M. W. Pospieszalski, "Cylindrical dielectric resonators and their applications in TEM line microwave circuits," *IEEE Trans. Microwave Theory Tech.*, vol. MTT-27, pp. 233-238, Mar. 1979.
- [22] T. Itoh and R. Rudokas, "New method for computing the resonant frequencies of dielectric resonators," *IEEE Trans. Microwave Theory Tech.*, vol. MTT-25, pp. 52-54, Jan. 1977.
- [23] M. Jaworski and M. W. Pospieszalski, "An accurate solution of the cylindrical dielectric resonator problem," *IEEE Trans. Microwave Theory Tech.*, vol. MTT-27, pp. 639-643, July 1979.

†

**M. Mohammad Taheri** was born in Saryazz, Yazd, Iran. He received the B.Sc. degree in electronic engineering from Sharif University of Technology, Tehran, Iran, in 1979 and the M.Sc. degree in telecommunication systems from the University of Essex, England, in 1986.



Between 1980 and 1982 he taught courses on propagation and antennas, electricity, and applied mathematics at Vatanpour Engineering Institute in Esfahan, Iran. Between 1982 and 1985 he worked at the Iran Telecommunication Company (ITC) and Iran Telecommunication Research Center (ITRC) as a development engineer, where he was involved in the design of microwave link and radio relay systems. At present, he is working towards the Ph.D. degree in the area of multimode dielectric-loaded cavity filters at the University of Essex, Colchester, England.

‡

**D. Mirshekar-Syahkal** received the B.Sc. degree (with distinction) in electrical engineering from Tehran University, Tehran, Iran, in 1974. He then received the M.Sc. degree in microwaves and modern optics in 1975 and the Ph.D. degree in 1979, both from University College London, London, England.



From 1979 to 1984, he carried out research on the characterization of millimeter-band planar transmission lines and the nondestructive evaluation of metals by electromagnetic techniques at the University College London. Since 1984, he has been on the staff at the University of Essex, Colchester, England, where he is a lecturer. His current research work is with problems of electromagnetic theory associated with passive microwave planar structures, the design of compact cavity filters, and the characterization of flaws in metals.

Dr. Mirshekar is a member of the Institute of Electrical Engineers and is a chartered engineer.